

Model predictive control design for multivariable processes in the presence of valve stiction*

Riccardo Bacci di Capaci^{a,b}, Marco Vaccari^a, Gabriele Pannocchia^a

^aDepartment of Civil and Industrial Engineering, University of Pisa, Pisa, Italy

^be-mail: riccardo.bacci@ing.unipi.it

Abstract

This paper presents different formulations of Model Predictive Control (MPC) to handle static friction in control valves for industrial processes. A fully unaware formulation, a stiction embedding structure, and a stiction inversion controller are considered. These controllers are applied to multivariable systems, with linear and nonlinear process dynamics. A semiphysical model is used for valve stiction dynamics and the corresponding inverse model is derived and used within the stiction inversion controller. The two-move stiction compensation method is revised and used as warm-start to build a feasible trajectory for the MPC optimal control problem. Some appropriate choices of objective functions and constraints are used with the aim of improving performance in set-points tracking. The different MPC formulations are reviewed, compared, and tested on several simulation examples. Stiction embedding MPC proves to guarantee good performance in set-points tracking and also stiction compensation, at the expense of a lower robustness with respect to other two formulations.

Keywords: Model predictive control, control valves, static friction, stiction modeling and compensation.

1. Introduction

Control valves are the most commonly used actuators in the process industries. Unfortunately, in many cases valves not only contain static nonlinearity (e.g. saturation), but also dynamic nonlinearity including backlash, friction, and hysteresis. Deadband due to backlash and mostly static friction (stiction) is a typical root source of the valve problems. A control valve with excessive deadband may not even respond to small changes in control action. As a result, these malfunctions may produce sustained oscillations in process variables, decrease the life of control valves, and generally, lead to inferior quality end-products causing reduced profitability of the whole industrial plant [2]. Hence, it appears that the potential benefits of using advanced control algorithms, as model predictive control (MPC), could be diminished because of poor valves, especially if their faults and malfunctions are not expressly considered in the plant model.

As a matter of fact, MPC has been used as an useful tool to improve control performance in the presence of various types of actuator faults, thus forming effective examples of fault tolerant control (FTC), as in [3] and [4]. In addition, MPC has been specifically applied as a compensation strategy for several types of control valve malfunctions. In particular, the first MPC-based formulation was developed in [5], using a mixed-integer quadratic programming (MIQP) on constraints of the input. An inverse backlash model and valve saturation are incorporated in the controller to overcome the deadband associated with backlash. Later, this structure has been applied to a

system with valve stiction in [6]. Due to the high computational burden and the resulting feedback effect, this approach may be inefficient in the case of severely nonlinear systems (high stiction) or highly dimensional systems. Further investigations of the same method in the case of valve stiction within the process, but not in the model, have been presented in [7].

Rodriguez and Heath [8] have proposed a formulation which reduces the bounds of optimization variables computed by the MPC, by trying to delete different types of valve nonlinearity, and by reducing the problem to a purely linear structure. The controller is indeed in series with a block that applies the inverse model for deadzone, backlash or stiction to the MPC output and sends this signal to the faulty valve, which can eventually saturate. Recently, Durand and Christofides [9] have presented an economic MPC structure which includes a detailed physical stiction model, constraints on the magnitude and rate of change of the input, and is combined with a slave controller of PI-type that regulates the valve output to its MPC set-point. This approach comprises a compensation strategy for nonlinear process systems, which can prevent the MPC from requesting physically unrealistic control actions due to stiction. Later, the same authors have replaced in [10] the first-principles model for the valve layer with a procedure for developing empirical models based only on data of valve set-point and flow rate. This approach incorporates a logic structure that activates different equations depending on the valve condition (that is, sticking or sliding phase): this forms a piecewise model where set-point changes may set which equations have to be chosen. The empirical model proves to be less stiff than the first-principles model and may improve the computation time with limited violations of process constraints.

*A preliminary version of this paper has been presented in [1].

As stated before, when stiction is present, the valve is not effective in following the command signal imposed by the controller. As a result, a limit cycle with sustained oscillations is typically produced in the proximity of the steady-state operating points. One way of reducing stiction effects is to explicitly take this malfunction into account in MPC design so that an improved performance could be obtained. As in many other fault tolerant control systems, where the fault estimate is crucial, for a good stiction tolerant MPC, a solid estimate of the stiction amount is needed, and the sticky valve must be properly located, especially when the system is multidimensional. For this purpose, well-established techniques of oscillation detection [11], and stiction diagnosis and quantification [12] could be used and adapted as necessary.

This paper is focused on designing and comparing different strategies of model predictive controller to handle static friction in control valve. Among three main different solutions, one MPC formulation considers valve stiction explicitly, using a semiphysical model [13] which is proved to give very close responses with respect to well-established first-principles models. The objective of this model-based approach is to compensate for the undesired effects of stiction on the controlled systems. Note that no method for valve stiction quantification has been expressly used or derived. Conversely, being stiction quantification beyond the scope of the paper, the amount of stiction is assumed as prior knowledge for predictive controllers.

The various controllers have been previously derived for single-input single-output (SISO) systems with linear process dynamics, as the nonlinearity came only from the valve [1]. In this work, the formulations have been refined and extended to multidimensional processes and nonlinear (and linearized) systems. An appropriate input sequence, derived from the two-move stiction compensation method and used as warm-start for MPC, is developed to improve set-point tracking performance. The considered MPC formulations are analyzed and compared using as test bench several simulation examples.

2. Problem definition

The whole multivariable plant is formed by the control valves followed by the process dynamics as shown in Figure 1. In detail, χ and y are the process input and output, that is, the valves output and the control variables, respectively; then, u is the MPC output, while w and v are white Gaussian noise. In [1]

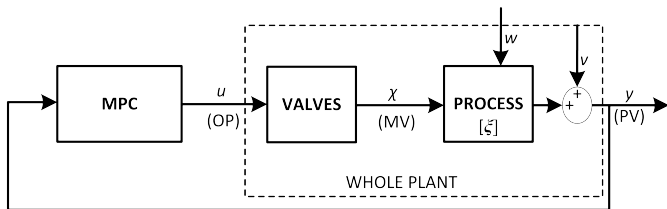


Figure 1: The closed-loop system with (sticky) control valves followed by the process.

the case of SISO system was studied. The system comprised a nonlinearity with memory for the valve followed by a linear

dynamics for the process, thus forming an extended Hammerstein structure for the whole plant. In this work, applications to MIMO systems with linear and nonlinear processes are presented.

In particular, the process dynamics is as follows:

$$\begin{aligned}\xi_{k+1} &= f_P(\xi_k, \chi_k) + w_k \\ y_k &= h_P(\xi_k) + v_k\end{aligned}\quad (1)$$

where variables are $\chi \in \mathbb{R}^m$, $u \in \mathbb{R}^m$, $y \in \mathbb{R}^p$, and $\xi \in \mathbb{R}^n$ (the process states), being n the model dimension; while functions are $f_P: \mathbb{R}^n \times \mathbb{R}^m \rightarrow \mathbb{R}^n$, $h_P: \mathbb{R}^n \rightarrow \mathbb{R}^p$. Whereas, the dynamics of the m valves is described by a data-driven stiction model:

$$\chi_k = \varphi(\chi_{k-1}, u_k) \quad (2)$$

expressed by the nonlinear function $\varphi: \mathbb{R}^m \times \mathbb{R}^m \rightarrow \mathbb{R}^m$, which is later discussed. Overall, the output of valve system χ represents the first m components of the state vector of the complete plant: $z_k = [\chi_{k-1}^T, \xi_k^T]^T$, so that $z \in \mathbb{R}^{n_z}$, being $n_z = m + n$. Therefore, the whole dynamics can be written as:

$$\begin{aligned}z_{k+1} &= \begin{bmatrix} \chi_k \\ \xi_{k+1} \end{bmatrix} = \phi_P(z_k, u_k) = \begin{bmatrix} \varphi(\chi_{k-1}, u_k) \\ f_P(\xi_k, \varphi(\chi_{k-1}, u_k)) + w_k \end{bmatrix} \\ y_k &= \zeta_P(z_k) + v_k\end{aligned}\quad (3)$$

where $\phi_P: \mathbb{R}^{n_z} \times \mathbb{R}^m \rightarrow \mathbb{R}^{n_z}$, and $\zeta_P: \mathbb{R}^{n_z} \rightarrow \mathbb{R}^p$, being $\zeta_P(z_k) = h_P(\xi_k)$. Note that in the present discussion, all actuators are assumed to be control valves, possibly affected by static friction. If some actuators are not valves, suitable simplifications can be easily made.

2.1. Proposed MPC approaches

Three different MPC approaches are presented and compared in this work. The first formulation is a “stiction unaware MPC”, with a partial nonlinear formulation since it completely disregards the valves dynamics and uses only the nonlinear process model for the whole plant (see Figure 2). Secondly, a “stiction embedding MPC” is considered, as shown in Figure 3. This controller is aware of the stiction presence, as it uses an extended model – comprised of valves and process dynamics – thus forming a full nonlinear formulation.

Finally, the third approach is also aware of stiction, but it has an explicit model for the inverse dynamics of stiction ($\tilde{\varphi}^{-1}$), as in Figure 4. In this case, \tilde{u} is the MPC output, subject to optimization, which forms input to stiction inverse model, and $u = \tilde{\varphi}^{-1}(\tilde{u})$ is the output of the whole controller. Note that, for a perfect stiction inversion, one get $\varphi(\tilde{\varphi}^{-1}(\tilde{u})) = \tilde{u}$, and then $\tilde{u} \equiv \chi$. This type of formulation, introduced by [8], has the advantage of considering expressly stiction dynamics, but it is mainly beneficial when the controller uses a linear model, that is, it is based on a linearized process dynamics.

2.2. Valve stiction modeling

For a healthy linear control valve, input (u) and output (χ) signals are equal (or at least proportional) at all times. But in the case of stiction, the valve acts like a nonlinear element and

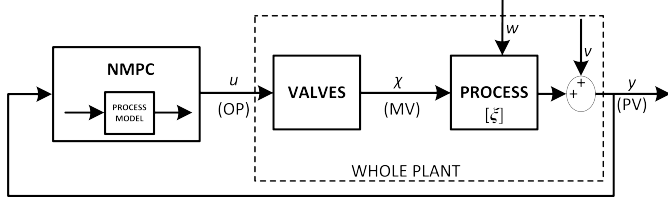


Figure 2: Closed-loop system with "stiction unaware MPC".

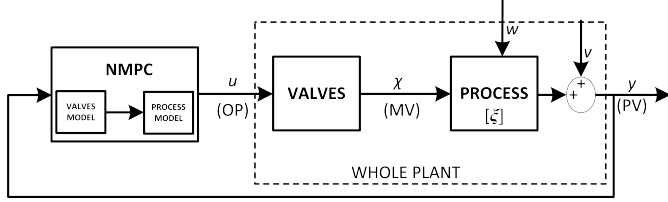


Figure 3: Closed-loop system with "stiction embedding MPC".

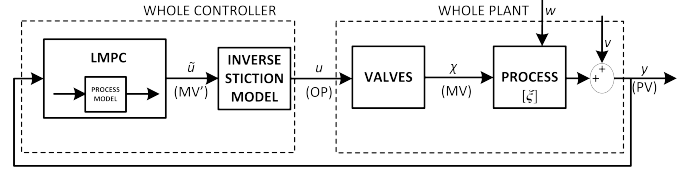


Figure 4: Closed-loop system with "stiction inversion MPC".

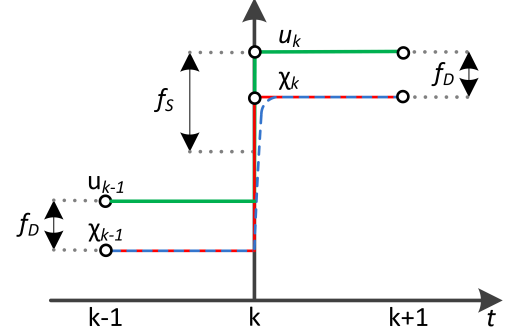


Figure 5: Steady-state approximation for valve stiction dynamics.

137 these two signals clearly differ. Note that stiction has been historically
 138 observed and studied in pneumatic globe valves with sliding stem and spring-diaphragm
 139 actuation system [2]. However, similar sticky behaviors can also occur in rotary pneumatic
 140 valves and even in electric control valves. Pneumatic and electric control valves differ
 141 actually only for the actuator, while the body and the plug, subjected to the majority of
 142 friction forces, can be exactly the same [14].

145 Stiction in control valves can be described both by detailed physical models, then by
 146 purely empirical models [15]. Physical models use Newton's second law of motion and
 147 classical forces balance on the valve. However, there are two main disadvantages of these
 148 first-principles models. Firstly, several physical parameters, also related to the valve's
 149 size, which are actually difficult to estimate, must be known. Secondly, computational
 150 times may be excessively long for practical purposes because cumbersome numerical
 151 integrations are necessary. Therefore, physical models are not often used in industrial
 152 applications.

156 On the other hand, data-driven (empirical) modeling approaches can get over the
 157 previous two drawbacks, by limiting the number of parameters and the computational
 158 burden. However, such models may also present some disadvantages. In fact, they
 159 cannot fully capture the dynamics of the valve, since, for example, not all the proposed
 160 models passed the specific open-loop tests applied by following the standards of
 161 International Society of Automation (ISA) [15].

164 When a fast response from the control valve is assumed, the transient behavior can be
 165 ignored, and a static – but with memory – nonlinear function can be used to approximate
 166 the valve's dynamic response, that is, only steady-state values of stem position are
 167 considered (see Figure 5). The standard empirical [16] or the semiphysical model [13]
 168 by He and coworkers are thus suitable to reproduce the valve response generated by
 169 physical stiction models without involving computationally intensive numerical
 170 integration.

173 *He's semiphysical stiction model.* In this paper, we choose to use He's semiphysical
 174 model [13], which includes stiction in

175 every valve movement, and reproduces accurately the valve signature obtained with the
 176 physical model in the case of low values of viscous friction F_v [13]. As said, preliminary
 177 version of this study has been carried out in [1] using He's standard model. 178

The flowchart of He's semiphysical model is given in Figure 6. The generic i -th sticky
 179 valve has nonlinear dynamics with memory $\chi_k^{(i)} = \varphi(\chi_{k-1}^{(i)}, u_k^{(i)})$, expressed by the
 180 following two relations:

$$181 \chi_k^{(i)} = \begin{cases} \chi_{k-1}^{(i)} + M \cdot [e_k^{(i)} - \text{sign}(e_k^{(i)}) f_D^{(i)}] & \text{if } |e_k^{(i)}| > f_S^{(i)} \\ \chi_{k-1}^{(i)} & \text{if } |e_k^{(i)}| \leq f_S^{(i)} \end{cases} \quad (4)$$

182 for $i = 1, \dots, m$, being m the number of valves, where $f_S^{(i)}$ and $f_D^{(i)}$ are static and
 183 dynamic friction parameters, respectively, and $e_k^{(i)} = u_k^{(i)} - \chi_{k-1}^{(i)}$. Note that $e_k^{(i)}$ is a
 184 sort of valve position error, and $f_S^{(i)} \geq f_D^{(i)}$ by definition. 185

The parameter M , which accounts for the overshoot observed in the physical model,
 186 can be assumed as a constant ($M = 1.99$) for different valve physical parameters
 187 when $F_v \simeq 0$ [13]. Therefore, this three-parameter model reduces to a modified
 188 version of the standard two-parameter model of He, and by 187

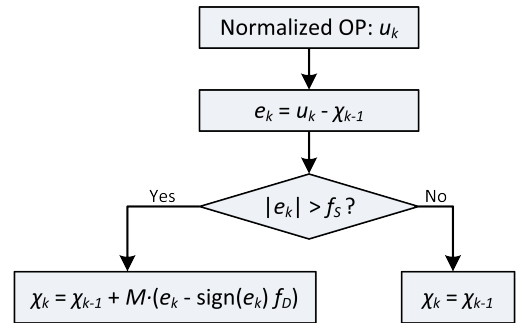


Figure 6: He's semiphysical stiction model [13].

188 imposing $M = 1$ the semiphysical model becomes exactly the
 189 standard one [16]. Nevertheless, it has to be noted that the semi-
 190 physical model is inconsistent in the case of no stiction, since
 191 for $f_S = f_D = 0$ valve input and output do not match perfectly.
 192 Hence, in this case, $\chi_k^{(i)} = u_k^{(i)}, \forall k$ should be directly imposed.

For the purpose of the work, after some simple algebra, (4) can be rewritten as:

$$\chi_k^{(i)} = \begin{cases} M(u_k^{(i)} - f_D^{(i)}) + \chi_{k-1}^{(i)}(1-M) & \text{if } u_k^{(i)} - \chi_{k-1}^{(i)} > f_S^{(i)} \\ M(u_k^{(i)} + f_D^{(i)}) + \chi_{k-1}^{(i)}(1-M) & \text{if } u_k^{(i)} - \chi_{k-1}^{(i)} < -f_S^{(i)} \\ \chi_{k-1}^{(i)} & \text{if } |u_k^{(i)} - \chi_{k-1}^{(i)}| \leq f_S^{(i)} \end{cases} \quad (5)$$

193 Therefore, the stiction nonlinearity φ in (3) is formed by a set
 194 of three linear and parallel relations for each valve, thus consti-
 195 tuting a sort of switching ‘‘multi-mode’’ model to be considered
 196 along with the dynamics of the process, to form a *discontinuous*
 197 model. Finally, it has to be noted that the proposed methodol-
 198 ogy and formulations of MPC could be derived also with other
 199 types of data-driven stiction models, as [17, 18].

200 3. MPC controller design

201 In this section the considered formulations of MPC are de-
 202 tailed, by introducing an empirical stiction inverse model, some
 203 specific choices for modules and tuning parameters, and a suit-
 204 able warm-start based on a stiction compensation method.

205 3.1. Stiction inverse model

206 The ‘‘stiction inverse MPC’’ formulation presented in Fig-
 207 ure 4 requires to invert the stiction nonlinearity to obtain the
 208 control sequence, that is, $u = \tilde{\varphi}^{-1}(\tilde{u})$. Starting from He’s semi-
 209 physical model in (5), by assuming $\tilde{u} = \chi$ and knowing at each
 210 sampling \tilde{u}_k and \tilde{u}_{k-1} , which compose inputs to the stiction
 211 inverse model, one can write that:

- if $\tilde{u}_k^{(i)} \neq \tilde{u}_{k-1}^{(i)}$ then:

$$u_k^{(i)} = \begin{cases} \frac{1}{M}[\tilde{u}_k^{(i)} + Mf_D^{(i)} - \tilde{u}_{k-1}^{(i)}(1-M)] & \Leftrightarrow u_k^{(i)} - \tilde{u}_{k-1}^{(i)} > f_S^{(i)} \\ \frac{1}{M}[\tilde{u}_k^{(i)} - Mf_D^{(i)} - \tilde{u}_{k-1}^{(i)}(1-M)] & \Leftrightarrow u_k^{(i)} - \tilde{u}_{k-1}^{(i)} < -f_S^{(i)} \end{cases}$$

- if $\tilde{u}_k^{(i)} = \tilde{u}_{k-1}^{(i)}$ then $u_k^{(i)} \in [\tilde{u}_{k-1}^{(i)} - f_S^{(i)}, \tilde{u}_{k-1}^{(i)} + f_S^{(i)}]$

Then, by substituting the expression of $u_k^{(i)}$ in the two inequalities, one gets:

$$u_k^{(i)} = \begin{cases} \tilde{U}_k^{(i)} + f_D^{(i)} & \text{if } \tilde{u}_k^{(i)} - \tilde{u}_{k-1}^{(i)} > M(f_S^{(i)} - f_D^{(i)}) \\ \tilde{U}_k^{(i)} - f_D^{(i)} & \text{if } \tilde{u}_k^{(i)} - \tilde{u}_{k-1}^{(i)} < -M(f_S^{(i)} - f_D^{(i)}) \\ \in [\tilde{u}_{k-1}^{(i)} - f_S^{(i)}, \tilde{u}_{k-1}^{(i)} + f_S^{(i)}] & \text{if } \tilde{u}_k^{(i)} - \tilde{u}_{k-1}^{(i)} = 0 \\ \text{is undefined} & \text{otherwise} \end{cases} \quad (6)$$

where $\tilde{U}_k^{(i)} = \frac{1}{M}[\tilde{u}_k^{(i)} - \tilde{u}_{k-1}^{(i)}(1-M)]$. Figure 7 shows a schematic representation of the function $\tilde{\varphi}^{-1}$ for the i -th valve. This stiction inverse model has an incomplete domain in \mathbb{R} , it admits unique values for $\tilde{u}_k - \tilde{u}_{k-1} > M(f_S - f_D) \geq 0$ and for $\tilde{u}_k - \tilde{u}_{k-1} < -M(f_D - f_S) \leq 0$, it is multivalued for $\tilde{u}_k - \tilde{u}_{k-1} = 0$, while otherwise is not defined. Note that, to implement this

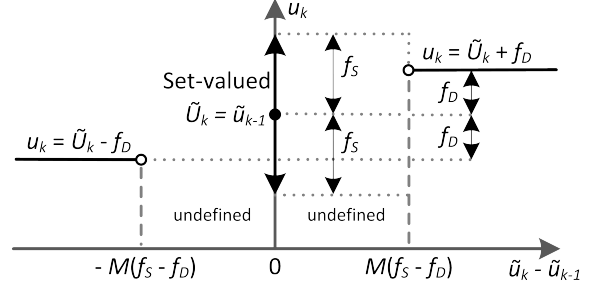


Figure 7: Inverse function $\tilde{\varphi}^{-1}$ for He’s semiphysical stiction model.

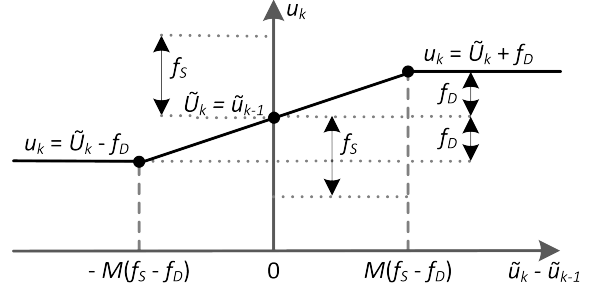


Figure 8: Approximated inverse function $\tilde{\varphi}^{-1}$ for He’s semiphysical stiction model.

exact model of stiction inverse in the MPC formulation, one should theoretically impose the following nonconnected domain \tilde{U} for values of \tilde{u}_k :

$$\tilde{U} = \left\{ \tilde{u}_k : \begin{aligned} &\tilde{u}_k^{(i)} > \tilde{u}_{k-1}^{(i)} + M(f_S^{(i)} - f_D^{(i)}) \cup \\ &\tilde{u}_k^{(i)} < \tilde{u}_{k-1}^{(i)} - M(f_S^{(i)} - f_D^{(i)}) \cup \\ &\tilde{u}_k^{(i)} = \tilde{u}_{k-1}^{(i)}, \forall i = 1, \dots, m \end{aligned} \right\} \quad (7)$$

which is not actually implementable, since it implies a nonconnected set of constraints on \tilde{u}_k , apart from the special case of pure deadband, that is, $f_S^{(i)} = f_D^{(i)} \forall i$. Therefore, an approximated inverse model ($\hat{\varphi}^{-1} \approx \tilde{\varphi}^{-1}$) is needed to implement a standard MPC. A possible simple solution is to turn the model into a continuous function with linear junctions, as the following:

$$u_k^{(i)} = \begin{cases} \tilde{U}_k^{(i)} + f_D^{(i)} & \text{if } \tilde{u}_k^{(i)} - \tilde{u}_{k-1}^{(i)} > M(f_S^{(i)} - f_D^{(i)}) \\ \tilde{U}_k^{(i)} - f_D^{(i)} & \text{if } \tilde{u}_k^{(i)} - \tilde{u}_{k-1}^{(i)} < -M(f_S^{(i)} - f_D^{(i)}) \\ \tilde{U}_k^{(i)} + \frac{f_D^{(i)}}{M(f_S^{(i)} - f_D^{(i)})} (\tilde{u}_k^{(i)} - \tilde{u}_{k-1}^{(i)}) & \text{if } |\tilde{u}_k^{(i)} - \tilde{u}_{k-1}^{(i)}| \leq M(f_S^{(i)} - f_D^{(i)}) \end{cases} \quad (8)$$

Figure 8 shows a schematic representation of this approximated stiction inverse for i -th valve. Note that for $f_S^{(i)} = f_D^{(i)}$ the third condition, that is, when $\tilde{u}_k^{(i)} - \tilde{u}_{k-1}^{(i)} = 0$, has to be reduced to $u_k^{(i)} = \tilde{U}_k^{(i)}$.

Extensive simulations have verified that approximated model (8) equals the exact one (6), that is, $\hat{\varphi}^{-1} \equiv \tilde{\varphi}^{-1}$, only when the difference $\tilde{u}_k^{(i)} - \tilde{u}_{k-1}^{(i)}$ is always within the domain of the exact inverse, and then one gets $\tilde{u}^{(i)} \equiv \chi^{(i)}$. Otherwise, the stiction inverse MPC formulation has a structural mismatch and its per-

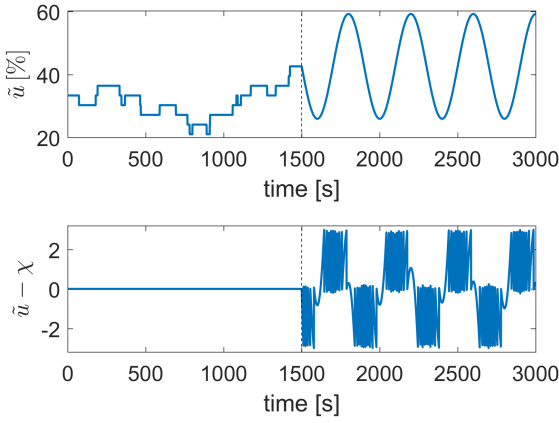


Figure 9: Behavior of stiction inverse model for a test signal ($f_S = 3$, $f_D = 1.5$).

222 performance tends to degrade. Figure 9 shows a test input $\tilde{u}^{(i)}$ to
 223 stiction inverse model. This signal belongs to \tilde{U} in (7) until
 224 1500 s and thus allows a perfect stiction inversion. Then, once
 225 the signal $\tilde{u}^{(i)}$ assumes the shape of a sine curve and does not
 226 belong to \tilde{U} , the stiction inversion becomes incomplete and the
 227 process input $\chi^{(i)}$ differs from the controller output $\tilde{u}^{(i)}$.

228 3.2. Other features of the MPCs selected for comparison

229 In this section the main features common to all formulations
 230 of MPC presented in Section 2.1 are detailed. A canonical
 231 offset-free MPC is used for all three formulations, as shown
 in Figure 10 [19].

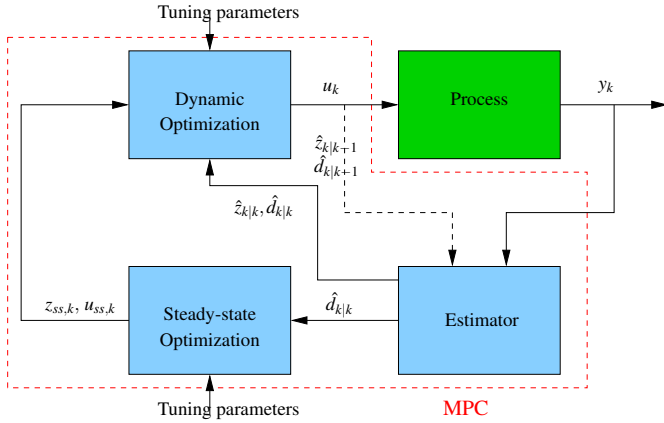


Figure 10: Scheme of offset-free MPC used in proposed formulations.

232 For all three formulations an input disturbance model is used.
 The stiction embedding MPC uses a full nonlinear structure, so
 that the augmented plant model becomes:

$$\begin{aligned}
 \hat{z}_{k+1|k} &= \phi(\hat{z}_{k|k}, u_k, \hat{d}_{k|k}) = \begin{bmatrix} \phi(\hat{\chi}_{k-1}, u_k) \\ f(\hat{\xi}_{k|k}, \phi(\hat{\chi}_{k-1}, u_k) + \hat{d}_{k|k}) \end{bmatrix} \\
 \hat{d}_{k+1|k} &= \hat{d}_{k|k} \\
 \hat{y}_k &= \zeta(\hat{z}_{k|k-1})
 \end{aligned} \quad (9)$$

where $\hat{d} \in \mathbb{R}^{n_d}$ is the estimate of input disturbance, where $n_d = m$. The stiction unaware MPC uses an incomplete nonlinear

structure, since stiction nonlinearity is unmodeled ($z \rightarrow \xi$, $\phi \rightarrow f$, $\zeta \rightarrow h$):

$$\begin{aligned}
 \hat{\xi}_{k+1|k} &= f(\hat{\xi}_{k|k}, u_k + \hat{d}_{k|k}) \\
 \hat{d}_{k+1|k} &= \hat{d}_{k|k} \\
 \hat{y}_k &= h(\hat{\xi}_{k|k-1})
 \end{aligned} \quad (10)$$

For stiction inversion MPC, a linearized model is used, with $z \rightarrow \xi$, $\phi \rightarrow f$ and $\zeta \rightarrow h$, so that:

$$\begin{aligned}
 \hat{\xi}_{k+1|k} &= A \hat{\xi}_{k|k} + B u_k + B_d \hat{d}_{k|k} \\
 \hat{d}_{k+1|k} &= \hat{d}_{k|k} \\
 \hat{y}_k &= C \hat{\xi}_{k|k-1}
 \end{aligned} \quad (11)$$

233 being $A = D_{\xi} f(\hat{\xi}) \in \mathbb{R}^{n \times n}$ and $B = D_u f(u) \in \mathbb{R}^{n \times m}$ the Jac-
 234 cobian matrices of state dynamics with respect to states ξ and
 235 input u , respectively; $C = D_{\xi} h(\hat{\xi}) \in \mathbb{R}^{p \times n}$ is the Jacobian ma-
 236 trix of output dynamics with respect to states ξ , and $B_d \in \mathbb{R}^{n \times n_d}$
 237 is the state disturbance matrix. The standard linear input distur-
 238 bance model is used: $B_d = B$.

239 The three modules (*Estimator*, *Steady-State Optimizer*, *Dy-*
 240 *namical Optimizer*) implemented in the proposed MPC formu-
 241 lations are briefly described below. Note that all modules are exe-
 242 cuted at each sample time given that the disturbance estimate \hat{d}
 243 is updated at each time k , and this implies that new targets need
 244 to be recomputed.

State estimation. The state estimator receives current output measurement (y_k) and predictions of state ($\hat{z}_{k|k-1}$) and disturbance ($\hat{d}_{k|k-1}$). The prediction update is made by:

$$\begin{bmatrix} \hat{z}_{k|k} \\ \hat{d}_{k|k} \end{bmatrix} = \begin{bmatrix} \hat{z}_{k|k-1} \\ \hat{d}_{k|k-1} \end{bmatrix} + K_k e_k \quad (12)$$

where $e_k = y_k - \hat{y}_k$ is the prediction error, and K_k is the observer gain matrix in $\mathbb{R}^{(n_z+n_d) \times p}$. The *Extended Kalman filter*, a classical dynamic observer, is used. Therefore, at each sample time k , the observer gain matrix K_k is computed by solving the following equations:

$$\begin{aligned}
 K_k &= (P_{k|k-1} C_k^T) (C_k P_{k|k-1} C_k^T + R_{kf})^{-1} \\
 P_k &= (I - K_k^T C_k)^T P_{k|k-1} \\
 P_{k+1|k} &= A_k P_k A_k^T + Q_{kf}
 \end{aligned} \quad (13)$$

245 where A_k and C_k are the Jacobian matrices of the augmented
 246 model dynamics and of the output map with respect to the
 247 augmented state vector $[z^T, d^T]^T$; $R_{kf} \in \mathbb{R}^{p \times p}$ and $Q_{kf} \in$
 248 $\mathbb{R}^{n_z+n_d \times n_z+n_d}$ are the measurements noise and process noise co-
 249 variance matrices, respectively; $P_0 \in \mathbb{R}^{n_z+n_d \times n_z+n_d}$ is the co-
 250 variance of the state error at the initial time. It is then imposed
 251 $R_{kf} = R_{wn}$, that is, estimated noise covariance matrix equals its
 252 actual value.

Steady-state optimization. The steady-state optimizer computes the state (z_{ss}), input (u_{ss}), and output (y_{ss}) targets to follow the desired external set-points (u_{sp} , y_{sp}) while respecting the imposed constraints. The optimization problem is as follows:

$$(z_{ss}, u_{ss}, y_{ss}) = \arg \min_{z, u, y} \ell_{ss}(u, y) \quad (14)$$

subject to:

$$\begin{aligned} z_{\min} &\leq z \leq z_{\max} \\ u_{\min} &\leq u \leq u_{\max} \\ y_{\min} &\leq y \leq y_{\max} \\ c_{ss}(z, u, y, \hat{d}_{k|k}) &= 0 \end{aligned} \quad (15)$$

The objective function is quadratic:

$$\ell_{ss}(u, y) = (y - y_{sp})^T Q_{ss} (y - y_{sp}) + (u - u_{sp})^T R_{ss} (u - u_{sp}) \quad (16)$$

where $Q_{ss} \in \mathbb{R}^{p \times p}$ is the output penalty matrix and $R_{ss} \in \mathbb{R}^{m \times m}$ is the control penalty matrix. The considered constraints are:

- *Bounds:* on state, input, and output vectors;
- *Equilibrium point* $c_{ss}(z, u, y, \hat{d}_{k|k})$: on the state map and on the output map, depending on (9), (10), or (11).

Dynamic optimization. The dynamic optimizer finds optimal trajectory (\mathbf{z}, \mathbf{u}) from current state and input to targets and computes $u_k = \mathbf{u}_k(0)$. The problem is formulated as follows:

$$[\mathbf{z}_k, \mathbf{u}_k] = \arg \min_{\mathbf{z}, \mathbf{u}} \ell_{dyn}(\mathbf{z}, \mathbf{u}) = \sum_{i=0}^{N-1} \ell(z_i, u_i) + V_f(z_N) \quad (17)$$

subject to:

$$\begin{aligned} z_{\min} &\leq z_i \leq z_{\max} \\ u_{\min} &\leq u_i \leq u_{\max} \\ \Delta u_{\min} &\leq \Delta u_i \leq \Delta u_{\max} \\ y_{\min} &\leq y_i \leq y_{\max} \\ z_0 &= \hat{z}_{k|k} \\ c_{eq}(z_i, z_{i+1}, u_i, y_i, \hat{d}_{k|k}) &= 0 \end{aligned} \quad (18)$$

where N is the prediction horizon, and $V_f(z_N) = (z_N - z_{ss})^T Q_N (z_N - z_{ss})$ is the terminal weight, with $Q_N \in \mathbb{R}^{n_z \times n_z}$. Also this objective function is quadratic:

$$\begin{aligned} \ell(z_i, u_i) &= (z_i - z_{ss})^T Q (z_i - z_{ss}) + \\ &+ (u_i - u_{ss})^T R (u_i - u_{ss}) + \Delta u_i^T S \Delta u_i \end{aligned} \quad (19)$$

where $Q \in \mathbb{R}^{n_z \times n_z}$ is the state penalty matrix, $R \in \mathbb{R}^{m \times m}$ is the control penalty matrix, $\Delta u_i = u_i - u_{i-1}$ is the input rate of change, and $S \in \mathbb{R}^{m \times m}$ is the control difference penalty matrix. The considered constraints are:

- *Bounds:* on the state, input, input rate of change, and on output;
- *Dynamic map* $c_{eq}(z_i, z_{i+1}, u_i, y_i, \hat{d}_{k|k})$: on the state map and on the output map, depending on (9), (10), or (11).

Controller tuning. Some general details about tuning parameters are given, even though specific numerical values depend on the various case studies. In the case of valve stiction, steady-state matrices can be chosen as $Q_{ss} = I_p$ and $R_{ss} = 0$, so that deviations from targets of inputs u_{ss} are not weighted at all. This choice is appropriate because valve stiction dynamics (5) admits multiple steady-states; in particular, when the valve is sticking, for a given steady output a range of inputs of width of $2f_S$ is possible, that is, $u_{ss} \in [\chi_{ss} - f_S, \chi_{ss} + f_S]$.

For stiction embedding MPC, the state penalty matrix Q can be chosen as a pure diagonal matrix with higher values in the first m elements in order to weigh deviations from steady-state position of valves. For both stiction embedding and stiction inversion MPC formulations, the following constraints on input rate of change are considered: $\Delta u_{\min, \max} = \mp a f_S$, where $a > 2$.

3.3. A suitable warm-start for stiction embedding MPC

In order to get good tracking performance and move variables to their targets by avoiding sustained oscillations induced by valve stiction, a suitable *warm-start* should be given to the dynamic optimizer of MPC. A general formulation of warm-start can be obtained by solving the following dynamic optimization problem:

$$\min_{\hat{\chi}_k, \hat{\chi}_{k+1}, u_{k+j}} (\hat{\chi}_{k-1} - \hat{\chi}_k)^2 + (\hat{\chi}_k - \hat{\chi}_{k+1})^2 + (\hat{\chi}_{k+1} - \hat{\chi}_{ss})^2 \quad (20)$$

subject to:

$$\begin{aligned} \hat{\chi}_k &= \varphi(\hat{\chi}_{k-1}, u_k) \\ \hat{\chi}_{k+1} &= \varphi(\hat{\chi}_k, u_{k+1}) \\ \hat{\chi}_{ss} &= \varphi(\hat{\chi}_{k+1}, u_{k+2}) \\ \hat{\chi}_{ss} &= \varphi(\hat{\chi}_{ss}, u_{k+3}) \end{aligned} \quad (21)$$

where $j = 0, \dots, 3$. The problem computes four moves ($u_k, u_{k+1}, u_{k+2}, u_{k+3}$) by optimizing on $\hat{\chi}_k$ and $\hat{\chi}_{k+1}$, and by assuming $\hat{\chi}_{k+3} = \hat{\chi}_{k+2} = \hat{\chi}_{ss}$.

In the proposed formulation (3), the valves output represent the first m components of the state vector of the complete plant model. Therefore, at each sampling time, the steady-state optimization module of stiction embedding MPC (9) can compute a suitable steady-state target (χ_{ss}) also for the valves output:

$$z_{ss} = \phi(z_{ss}, u_{ss}) = \begin{bmatrix} \chi_{ss} \\ \xi_{ss} \end{bmatrix} = \begin{bmatrix} \varphi(\chi_{ss}, u_{ss}) \\ f(\xi_{ss}, \varphi(\chi_{ss}, u_{ss})) \end{bmatrix} \quad (22)$$

$$y_{ss} = \zeta(z_{ss}) = y_{sp}$$

Alternatively, a particular input sequence could be used as first-guess trajectory. This suitable warm-start is inspired by a new version of the two-move stiction compensation method. Introduced by [20], the ‘‘two-move compensator’’ ought to remove oscillations on control variable, and keep the valve output at its steady-state value, by performing at least two moves in opposite directions. Afterwards, further and improved implementations of stiction compensators based on this approach have been then developed in [21], [22], and [23].

In this work, the following sequence is given as warm-start to input signal of each m valve on the basis of semiphysical He's stiction model (5):

$$\begin{aligned}
u_k &= \begin{cases} u_{k-1} + af_s & \text{if } u_{k-1} \geq \chi_{ss} \\ u_{k-1} - af_s & \text{if } u_{k-1} < \chi_{ss} \end{cases} \\
u_{k+1} &= \begin{cases} \chi_k + f_D & \text{if } u_k \geq \chi_k \\ \chi_k - f_D & \text{if } u_k < \chi_k \end{cases} \\
u_{k+2} &= \begin{cases} X_{k+2} - f_D & \text{if } u_{k+1} \geq \chi_{ss} \\ X_{k+2} + f_D & \text{if } u_{k+1} < \chi_{ss} \end{cases} \\
u_{k+3} &= \begin{cases} \chi_{k+2} + f_D & \text{if } u_{k+2} \geq \chi_{k+2} \\ \chi_{k+2} - f_D & \text{if } u_{k+2} < \chi_{k+2} \end{cases} \\
u_{k+j} &= u_{k+3} (= u_{ss}) \quad \text{if } j > 3
\end{aligned} \tag{23}$$

where $X_{k+2} = \frac{1}{M}[\chi_{ss} - \chi_{k+1}(1-M)]$. The *first* input u_k (for $j = 0$) moves the valve stem away from its stuck position, if $a > 2$. By observing (5), it is evident that the maximum value of the difference between valve input and output that does not cause a movement in the valve is $|u_k - \chi_{k-1}| = f_s$. If $u_{k-1} \geq \chi_{ss}$, in the worst case $u_{k-1} - \chi_{k-1} = -f_s$. Therefore, if $a > 2$, one gets $|u_k - \chi_{k-1}| > f_s$ and moves the valve: $\chi_k \neq \chi_{k-1}$ (see Figure 11). Then, for the *second* movement u_{k+1} (for $j = 1$), the input is moved towards the actual valve position χ_k and set at a distance f_D , so that the valve does not move since the dependency of valve output with the previous value of χ is removed. The *third* signal u_{k+2} brings the stem position to its steady-state value (χ_{ss}) in order to eliminate error on control variable. Finally, the *fourth* movement u_{k+3} , analogously to the aim of the second move, moves towards the steady-state valve position and set the input at distance f_D , so that $\chi_{k+3} = \chi_{k+2} = \chi_{ss}$. After that, the stem cannot move from steady-state position since the input signal u_{k+j} (with $j > 3$) is always kept constant.

Note that (24) comprises actually a sequence of four moves, being based on He's semiphysical model. A simpler compensation sequence has been derived for He's standard model in [1], and indeed represents a regular two-move method, since it imposes only two different values to the valve input.

It is worth noting that the first version of two-move stiction compensation presented several drawbacks, which heavily hinder its on-line implementation [22]. Firstly, accuracy is reduced by assuming the one-parameter model of [24] to predict the valve behavior. Moreover, the steady-state value of valve position (χ_{ss}) is assumed to be known, while this variable is not usually measurable in process plants. In particular, the method relies on the strong assumption that all measurements are represented by deviation variables and their respective steady-state values are zero.

In the proposed warm-start (24), steady-state valve positions are estimated by (22), and, for transitory values of valve output (χ_k, χ_{k+1}), the estimates computed along the prediction horizon N are considered. This input sequence proves to be a valid *warm-start* for the stiction embedding MPC, by improving sig-

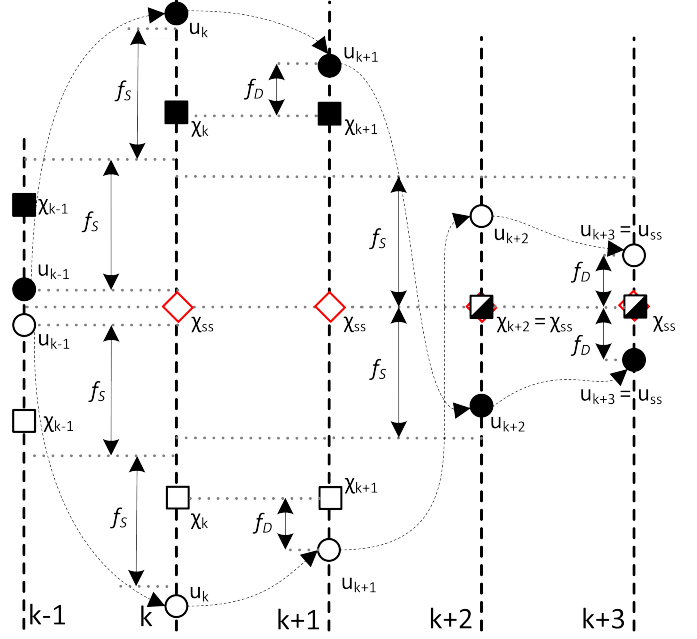


Figure 11: Sequence of moves for stiction compensation.

nificantly performance of the dynamic optimization module:

$$\begin{aligned}
u_{1:N}^0 &= [u_1^0, u_2^0, u_3^0, u_4^0, \dots, u_{N-1}^0, u_N^0] \\
&= [u_0 \pm af_s, \hat{\chi}_1 \pm f_D, \hat{X}_2 \pm f_D, \hat{\chi}_{ss} \pm f_D, \dots \\
&\quad \dots, \hat{\chi}_{ss} \pm f_D, \hat{\chi}_{ss} \pm f_D]
\end{aligned} \tag{24}$$

where $\hat{X}_2 = \frac{1}{M}[\hat{\chi}_{ss} - \hat{\chi}_1(1-M)]$.

The beneficial effect of the proposed warm-start is shown in the remainder of this section for a numerical case-study. Nominal performance is considered, since no error in process and valve dynamics is present, and no noise is added. A linear SISO system is considered for the sake of simplicity. Stiction is described by He's semiphysical model with $f_s = 5$ and $f_D = 2$. A third-order transfer function for the process model is considered:

$$P(s) = \frac{1}{(10s+1)(5s+1)(s+1)}$$

and the corresponding state-space model in discrete time domain with sampling period $T_s = 1$ is obtained. Four different scenarios are analyzed:

1. *standard stiction embedding MPC*: no warm-start is used;
2. *pure warm-start*: the dynamic module of stiction embedding MPC is bypassed and the controller output corresponds exactly to the warm-start sequence;
3. *stiction embedding MPC with warm-start*: the sequence in (24) is given as warm-start to the controller;
4. *improved stiction embedding MPC with warm-start*: the proposed warm-start is used and a revised objective function is introduced.

Figure 12 shows time trends of process output and valve position of the various scenarios for the same set-point. The standard stiction embedding MPC does not move the input, thus the

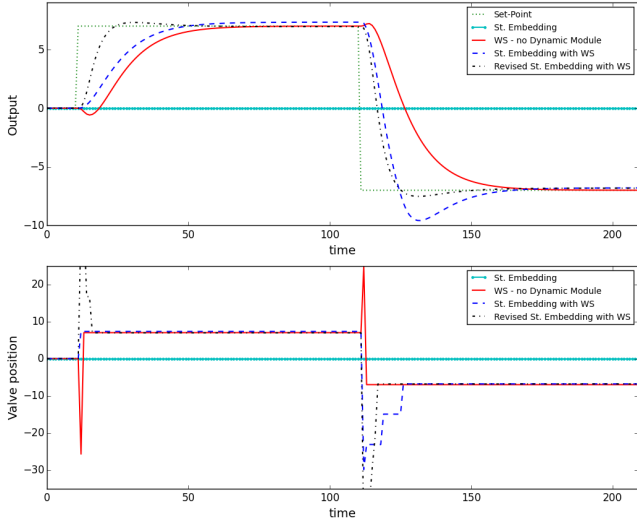


Figure 12: Beneficial of warm-start on stiction embedding MPC.

343 output does not reach the new set-point. The dynamic optimizer
 344 finds more convenient to stay at the initial steady-state, since,
 345 by modeling the valve deadband within the plant dynamics, the
 346 objective function could be diminished only along an unpractical
 347 prediction horizon ($\tilde{N} \approx 5 \cdot 10^4$ for this specific case). The
 348 pure warm-start excludes dynamic module of MPC and is basically
 349 open-loop mode control. This scenario allows one to get new
 350 reference with perfectly zero offset and new target for states,
 351 but with a very slow response.

The stiction embedding MPC with warm-start moves valve position when set-point changes occur, but may yield significant offsets as new targets cannot be matched always perfectly by dynamic module. Finally, in the improved stiction embedding MPC formulation, the dynamic objective function (17) is revised as follows:

$$\ell(z_i, u_i) = (z_i - z_{ss})^T Q (z_i - z_{ss}) + \Delta \hat{\chi}_i^T Q_s \Delta \hat{\chi}_i \quad (25)$$

352 where $\Delta \hat{\chi}_i = \hat{\chi}_i - \hat{\chi}_{i-1}$ is the rate of change of the estimated
 353 valve position, and $Q_s \in \mathbb{R}^{m \times m}$ is the corresponding difference
 354 penalty matrix. Note that matrices R and S in (17) have to be
 355 set to zero accordingly, since limitations on process input are
 356 now imposed directly on the estimated valve position and not on
 357 controller output. This refined approach further reduces offset
 358 and speeds up response, but at the expense of a larger input
 359 variation and wider valve movements in transitory dynamics.

360 Nevertheless, it has to be remarked that the proposed warm-
 361 start has a major limitation since it is effective only for constant
 362 set-point or in the case of pure step changes. As a matter of fact,
 363 the two-move compensation which is based on is actually suitable
 364 only in the case of constant set-point, that is, when a fixed
 365 steady-state value χ_{ss} of valve position is known, measured or
 366 estimated. In the case of step changes, targets of valves position,
 367 as other states, show step variations and proposed warm-
 368 start is still effective. However, degraded performance occur
 369 when set-point is time-varying and corresponding steady-state
 370 values of valves position change along the short horizon (four
 371 moves) of the warm-start.

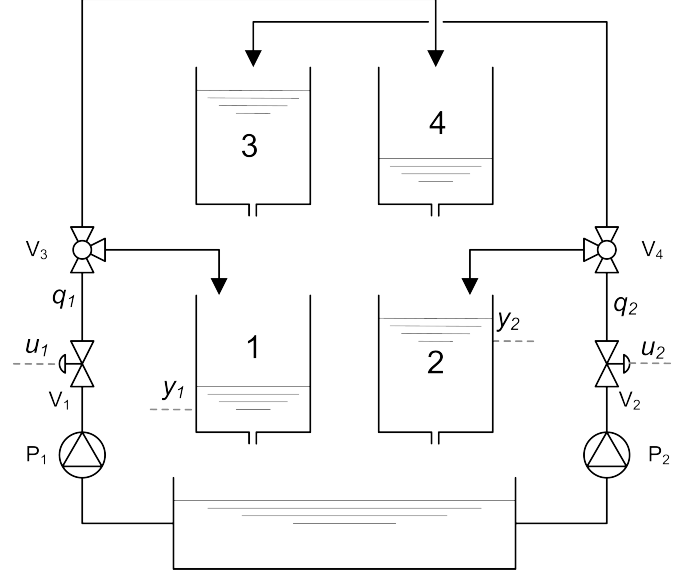


Figure 13: A multivariable nonlinear system: the quadruple-tank process.

4. Simulation analysis

The objective of this section is to investigate the performance of the three proposed formulations of MPC in order to compensate for valve stiction. Simulations are performed on a code adapted from [25], written in Python 2.7 with the use of symbolic framework offered by CasADi 3.1. Both optimization modules of MPC implement IPOPT as nonlinear programming solver.

4.1. Quadruple-tank process

An adaptation of the well-known quadruple-tank process [26] is here considered. A schematic diagram of the system is shown in Figure 13. The target is to control the level of the lower two tanks by means of two control valves (V_1, V_2). The process inputs are u_1 and u_2 , that is, the output signals from MPC, and the process outputs are y_1 and y_2 , level measurement of lower tanks, while level of upper tanks are assumed not measurable.

Mass balances and Bernoulli's law yield to the following continuous-time nonlinear process dynamics:

$$\begin{aligned} \frac{d\xi_1}{dt} &= -\frac{a_1}{A_1} \sqrt{2g\xi_1} + \frac{a_3}{A_1} \sqrt{2g\xi_3} + \frac{\gamma_1}{A_1} K_1 \chi_1 \\ \frac{d\xi_2}{dt} &= -\frac{a_2}{A_2} \sqrt{2g\xi_2} + \frac{a_4}{A_2} \sqrt{2g\xi_4} + \frac{\gamma_2}{A_2} K_2 \chi_2 \\ \frac{d\xi_3}{dt} &= -\frac{a_3}{A_3} \sqrt{2g\xi_3} + \frac{(1-\gamma_2)}{A_3} K_2 \chi_2 \\ \frac{d\xi_4}{dt} &= -\frac{a_4}{A_4} \sqrt{2g\xi_4} + \frac{(1-\gamma_1)}{A_4} K_1 \chi_1 \end{aligned} \quad (26)$$

where the meaning of all variables and parameters is detailed in Table 1.

The inlet flow to tank 1 is $\frac{\gamma_1}{A_1} K_1 \chi_1$, and the inlet flow to tank 4 is $\frac{(1-\gamma_1)}{A_4} K_1 \chi_1$. Analogously, inlet flows result for tank 2 and

Table 1: Variables and parameters of quadruple-tank process.

Parameter	Description [Unit]	Value
ξ_i	water level [cm]	-
χ_i	valve position [%]	-
g	acceleration of gravity [cm/s ²]	981.0
a_i	cross-section of the outlet hole [cm ²]	$a_1 = 0.071$
		$a_2 = 0.057$
		$a_3 = 0.071$
		$a_4 = 0.057$
A_i	cross-section of tank [cm ²]	$A_1 = 28.0$
		$A_2 = 32.0$
		$A_3 = 28.0$
		$A_4 = 32.0$
γ_i	flow splitting factor $\in (0, 1)$	$\gamma_1 = 0.7$
		$\gamma_2 = 0.6$
ξ_i^{max}	maximum tank level [cm]	$\xi_1^{max} = 20.0$
		$\xi_2^{max} = 20.0$
q_i^{max}	maximum flow rate [cm ³ /s]	$q_1^{max} = 2 \cdot a_1 \sqrt{2g\xi_1^{max}}$
		$q_2^{max} = 2 \cdot a_2 \sqrt{2g\xi_2^{max}}$
K_i	proportional constant, valve position vs. flow rate $\chi_i - q_i$; valves with linear characteristics	$K_1 = q_1^{max}/100$
		$K_2 = q_2^{max}/100$

tank 3. The modeling and control of the system have been studied at two operating points [26]. In this paper, only conditions with minimum-phase characteristics are investigated, when the control is easier and holds for $(\gamma_1, \gamma_2) > 0.5$. Control valve can be subject to stiction, which is described by He's semiphysical model (5). Valve V_1 is sticky, with $f_S^{(1)} = 6$, $f_D^{(1)} = 2$, $M = 1.99$, while valve V_2 is healthy, so that $\chi^{(2)} = u^{(2)}$. Note that stiction presence and amount are assumed known *a priori* for the plant model. Continuous-time dynamics of four tanks (26) is integrated using explicit Runge-Kutta 4th order method, in order to match discrete-time dynamics of two valves:

$$z_{k+1} = \begin{bmatrix} \chi_k \\ \xi_{k+1} \end{bmatrix} = \Phi_P(z_k, u_k) = \begin{bmatrix} \varphi(\chi_{k-1}, u_k) \\ f_P(\xi_k, \varphi(\chi_{k-1}, u_k)) \end{bmatrix} \quad (27)$$

$$y_k = C\xi_k + v_k = \begin{bmatrix} 1 & 0 & 0 & 0 \\ 0 & 1 & 0 & 0 \end{bmatrix} \xi_k + v_k$$

where valves output and tanks level compose the state vector of the complete plant $z_k = [\chi_{k-1}^T, \xi_k^T]^T$.

4.2. Nominal comparison

The three proposed formulations of MPC are compared under equivalent conditions in terms of state observer and disturbance model as discussed in Section 3.2. The prediction horizon and the sampling period are set to $N = 50$ and $T_s = 5s$. The major differences lay in the stiction compensation sequence of (24) and in the revised cost function of (25), which are respectively used within dynamic optimization module of the stiction embedding MPC formulation as warm-start and as objective function. Two different scenarios are studied:

- *nonlinear models*: the quadruple-tank model used within MPC formulations is nonlinear (26); only stiction unaware

MPC and stiction embedding MPC, which also implements valves nonlinearity, are derived.

- *linearized model*: the quadruple-tank model used within stiction inversion MPC is purely linear and the stiction nonlinearity $\varphi(\cdot)$ is inverted after optimization.

In this second scenario, the nonlinear dynamics of four tanks in (27) is linearized around the initial steady-state point $(\hat{\xi}_{ss}, \hat{\chi}_{ss})$:

$$A = D_{\hat{\xi}} f(\hat{\xi}_{ss}, \hat{\chi}_{ss}) = \begin{bmatrix} 0.9222 & 0 & 0.1958 & 0 \\ 0 & 0.9451 & 0 & 0.1479 \\ 0 & 0 & 0.7958 & 0 \\ 0 & 0 & 0 & 0.8477 \end{bmatrix},$$

$$B = D_{\hat{\chi}} f(\hat{\xi}_{ss}, \hat{\chi}_{ss}) = \begin{bmatrix} 0.0304 & 0.0019 \\ 0.0009 & 0.0231 \\ 0 & 0.0162 \\ 0.0110 & 0 \end{bmatrix} \quad (28)$$

where $D_{\hat{\xi}}(\cdot)$ and $D_{\hat{\chi}}(\cdot)$ are the Jacobians of process model dynamics with respect to tank levels $\hat{\xi}$ and valves position $\hat{\chi}$, and $\hat{\xi}_{ss} = [11.99, 12.19, 1.51, 1.42]$, and $\hat{\chi}_{ss} = [39.58, 38.15]$.

For all three formulations, tuning parameters of the static module and the terminal penalty matrix are the same: $Q_{ss} = I_2$, $R_{ss} = 0$, and $Q_N = 10^2 I_{n_z}$. Some differences lay in dynamic modules. In the case of stiction embedding (SE) MPC, $Q = \text{diag}[10^3, 10^3, 1, 1, 10^{-6}, 10^{-6}]$, $Q_S = \text{diag}[10, 100]$. For stiction unaware (SU) and stiction inversion (SI) MPC, $Q = \text{diag}[1, 1, 10^{-6}, 10^{-6}] \simeq C^T C$, $S = \text{diag}[10, 100]$, $R = \text{diag}[10^3, 10^3]$. Note that $C^T C = \text{diag}[1, 1, 0, 0]$, $Q_{(1:2, 1:2)}^{SE} = R^{SU, SI}$, and $Q_S^{SE} = S^{SU, SI}$, that is, tuning values are comparable among the three formulations.

Also a corresponding "ideal" MPC, with same tuning parameters, but under stiction-free environment has been considered. This nonlinear stiction-free formulation (NMPC-SF) is used as baseline for comparison, since stiction unaware MPC and stiction embedding MPC can be reduced to this controller in the absence of stiction. Figure 14 shows time trends of the tank levels, controller outputs, and valves position with different MPC formulations for the same set-points, comprised of sequences of step changes. Stiction embedding formulation can guarantee very good tracking performance with negligible offsets on both process variables, thus an effective stiction compensation is possible. Note that valve stiction is compensated so well to reproduce the behavior of the stiction unaware nonlinear controller in stiction-free environment (NMPC-SF). As a matter of fact, process outputs and valves position are substantially the same.

On the other hand, simple unaware MPC shows lower performance and does not usually remove oscillations induced by stiction, which propagate from sticky valve to all control variables. Similarly, even stiction inversion MPC, despite being aware of the valve malfunction, cannot yield good control, since the conditions (7) on input sequence to get a perfect stiction inversion, are not verified in closed-loop operation. Note that fluctuations produced by these two MPC formulations are caused by the disturbance estimate which is not zero, due to the unmodeled

448 – or miss-modeled – valve dynamics. Frequencies and ampli- 492
 449 tudes of oscillation may change during the same simulation, 493
 450 since a dynamic state observer is used. Therefore, the effects 494
 451 of a time-varying gain K_k (12) on stiction induced oscillations 495
 452 are similar to those of a change of proportional gain K_c in a 496
 453 traditional PID controller. Finally, note that controller retuning 497
 454 cannot completely remove these stable oscillations, but simply 498
 455 alters occurrences, amplitudes and frequencies. 499

456 A different version of stiction inversion MPC has also been 500
 457 tested. In order to fill the region where the exact inverse model 501
 458 $\tilde{\varphi}^{-1}$ is undefined, instead of the linear function used in $\hat{\varphi}^{-1}$ 502
 459 (Figure 8), a sigmoid function has been used. This modified 503
 460 version of stiction inversion model gives some little improve- 504
 461 ments, since lower amplitude and period fluctuations with re- 505
 462 spect to the original formulation can be obtained. However, 506
 463 this revised controller is not enough to give a complete stiction 507
 464 inversion and then to delete sustained oscillation. In the sake of 508
 465 space, the corresponding results are not reported. 509

466 It is also worth highlighting that the proposed fully-nonlinear 510
 467 formulation of stiction embedding MPC is more effective than 511
 468 a corresponding partly-nonlinear MPC, based on the linearized 512
 469 model (28), since plant-model mismatch is introduced by the 513
 470 linearization. A linearized stiction embedding MPC may ex- 514
 471 hibit non-negligible offsets since target calculation would be 515
 472 corrupted by linearization of four-tank dynamics, but detrimen- 516
 473 tal oscillations would be anyway avoided. In addition, non- 517
 474 negligible errors may be due to corruption of warm-start ef- 518
 475 ficiency, since targets would vary also after set-point changes 519
 476 due to model linearization. Finally, an eventual linearized for- 520
 477 mulation of stiction unaware MPC would exhibit fluctuations of 521
 478 similar amplitude and frequency than corresponding nonlinear 522
 479 controller. 523

480 4.3. Further results 524

481 Some further analyses are presented in this section. 525

Effect of noise. The noise effect is investigated by considering 526
 all the same parameters used in nominal analysis. Eight simu- 527
 lations are performed with different magnitude of the output 528
 white noise covariance matrix R_{wn} , where $v = R_{wn}^{1/2} v_{rnd}$, and v_{rnd} 529
 is a random sequence with normal distribution, zero-mean and 530
 unit standard deviation. The performance is evaluated using the 531
 following closed-loop objective function: 532

$$482 \quad J_{CL} = (y - y_{sp})^T (y - y_{sp}) + \Delta\chi^T S_p \Delta\chi \quad 533$$

$$483 \quad + (\chi - \chi^{SE})^T R_p (\chi - \chi^{SE}) \quad (29) \quad 534$$

484 where $S_p = Q_S$ in the case of stiction embedding MPC, while 535
 485 $S_p = S$ for stiction unaware and stiction inversion MPC; $R_p =$ 536
 486 $Q_{(1:2,1:2)}$ for stiction embedding MPC and $R_p = R$ for other two 537
 487 formulations. Note that χ and $\Delta\chi$ are the value and the rate 538
 488 of change of actual valves position and χ^{SE} is the actual valves 539
 489 position for a stiction embedding MPC in nominal scenario, that 540
 490 is, in the case of no noise and no error on plant dynamics. 541

489 Table 2 summarizes the overall results. It can be observed 542
 490 that for stiction unaware and stiction inversion MPC rather con- 543
 491 stant values of J_{CL} are obtained. The stiction embedding MPC 544
 545

492 produces lower values of J_{CL} only until $R_{wn} = 10^{-5}$, but shows 493
 494 a lower robustness to noise, since larger values are obtained 495
 496 as the noise increases with respect to other two formulations. 497
 498 Therefore, very good tracking performance and stiction com- 499
 500 pensation cannot be guaranteed for significant levels of noise, 501
 502 since non-negligible offset on controlled variables may occur. 503

Effect of mismatch on stiction parameters. Finally, the effect of 504
 505 wrong values of stiction parameters (\hat{f}_S, \hat{f}_D) in the valve model 506
 507 of two stiction aware MPC formulations – inversion and em- 508
 509 bedding – is studied. Actual values are $f_S = 6$, $f_D = 2$, and 509
 510 mismatched values on static and dynamic friction are consid- 510
 511 ered separately. In the first case, \hat{f}_S is varied; in the second, \hat{f}_D 511
 512 is changed. Figure 15 summarizes the whole results, by show- 512
 513 ing values of J_{CL} (29) with respect to single errors: $e_S = f_S - \hat{f}_S$ 513
 514 and $e_D = f_D - \hat{f}_D$. 514

515 For stiction embedding MPC, as expected, minimum values 516
 517 of the objective function are obtained for null errors. Whereas, 517
 518 performance can significantly degrade when stiction paramet- 518
 519 ers are wrong, underrated or overrated, as significant offsets on 519
 520 controlled variables may arise. Therefore, stiction embedding 520
 521 MPC proves to be stiction parameters dependent and is practi- 521
 522 cable only when stiction parameters are well known or in the 522
 523 case of slight uncertainties on valve stiction dynamics. Con- 523
 524 troller retuning could improve performance, but offsets might 524
 525 occur again when other operation conditions are imposed. On 525
 526 the other hand, stiction inversion MPC shows a higher value 526
 527 of performance index J_{CL} in the nominal case ($e_S, e_D = 0$), but 527
 528 this formulation has overall a much higher robustness to errors 528
 529 on stiction parameters. Oscillations occur in all scenarios, only 529
 530 frequencies and amplitudes may change. 530

523 5. Conclusions 524

523 This paper has presented three different formulations of MPC 524
 525 to handle static friction in control valves for industrial pro- 525
 526 cesses. A fully unaware formulation, a stiction embedding 526
 527 structure, and a stiction inversion controller are designed. These 527
 528 model predictive controllers have been applied to multivariable 528
 529 processes with nonlinear systems. 529

529 It is observed that stiction embedding nonlinear MPC is the 530
 530 only formulation which can guarantee good performance in set- 530
 531 points tracking and also stiction compensation. The two-move 531
 532 stiction compensation method is revised and used as warm-start 532
 533 to build a suitable trajectory for this MPC. In addition, some 533
 534 appropriate choices of objective functions and variables con- 534
 535 straints are used with the aim of further improving performance. 535
 536 Nevertheless, this controller can produce non-negligible offsets 536
 537 when stiction is still fully modeled, but a linearization of non- 537
 538 linear process dynamics is performed. In addition, a robust be- 538
 539 havior is not possible in the presence of significant amount of 539
 540 white noise on the output. A similar result arises in the case 540
 541 of errors in the valve dynamics, that is, mismatches on stiction 541
 542 parameters, since offsets on process variables may be relevant. 542

543 On the other hand, the other two MPC formulations show 544
 544 lower compensation performance and do not completely re- 544
 545 move oscillations induced by valve stiction in the nominal sce- 545

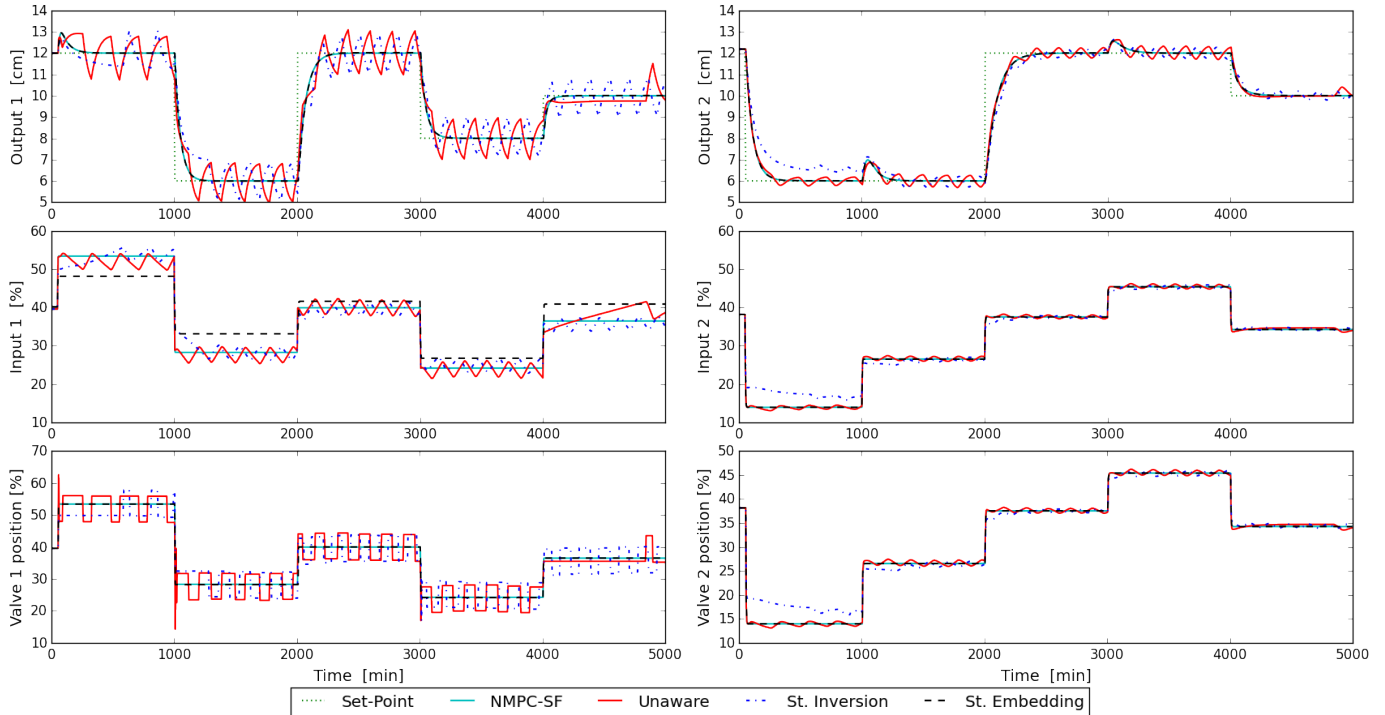


Figure 14: Nominal comparison. Tank levels, controller outputs, and valves position for three different MPC formulations.

Table 2: Effect of noise for three MPC formulations. Values of the objective function $J_{CL} [\times 10^7]$.

Noise Level (R_{wn})	0	10^{-9}	10^{-6}	10^{-5}	10^{-4}	10^{-3}	10^{-2}	0.1
SU-MPC	1.6510	1.8130	1.8908	1.5204	1.6556	1.8591	1.8925	1.8638
SI-MPC	1.7459	1.2992	1.3418	1.3434	1.5666	1.4930	1.3238	1.9481
SE-MPC	0.1009	0.1235	0.8343	1.2361	4.5288	7.1767	8.7153	8.4120

546 nario. Note that even stiction inversion MPC, despite being
 547 aware of the valve fault, cannot yield a good control, since con-
 548 ditions of discontinuity on input sequence to get perfect stic-
 549 tion inversion are hardly verified when this controller is imple-
 550 mented in closed-loop. Anyway, this formulation shows higher
 551 robustness to errors on stiction parameters, and frequencies and
 552 amplitudes of oscillation marginally change.

553 References

554 [1] R. Bacci di Capaci, M. Vaccari, G. Pannocchia, A valve stiction toler-
 555 ant formulation of MPC for industrial processes, in: Proceedings of the
 556 20th IFAC World Congress, Toulouse, France, 9–14 July, 2017, pp. 9374–
 557 9379.
 558 [2] M. Jelali, B. Huang, Detection and Diagnosis of Stiction in Control
 559 Loops: State of the Art and Advanced Methods, Springer-Verlag, Lon-
 560 don, 2010.
 561 [3] J. Tao, Y. Zhu, Q. Fan, Improved state space model predictive control
 562 design for linear systems with partial actuator failure, Ind. Eng. Chem.
 563 Res. 53 (2014) 3578–3586.
 564 [4] A. Alanqar, H. Durand, P. D. Christofides, Fault-tolerant economic model
 565 predictive control using error-triggered online model identification, Ind.
 566 Eng. Chem. Res. 56 (2017) 5652–5667.
 567 [5] H. Zabiri, Y. Samyudia, A hybrid formulation and design of model pre-
 568 dictive control for systems under actuator saturation and backlash, J. of
 569 Process Contr. 16 (2006) 693–709.

[6] H. Zabiri, Y. Samyudia, MIQP-based MPC in the presence of control
 570 valve stiction, Chemical Product and Process Modeling 4 (2009) 85–97.
 571 [7] B. Kamaruddin, H. Zabiri, Investigating MIQP-based MPC performance
 572 for stiction compensation, Australian Journal of Basic and Applied Sci-
 573 ences 9 (2015) 78–84.
 574 [8] M. Rodríguez, W. Heath, MPC for plants subject to saturation and dead-
 575 zone, backlash or stiction, in: Proceedings of the 4th IFAC Nonlinear
 576 Model Predictive Control Conference, Noordwijkerhout, The Nether-
 577 lands, 2012, pp. 418–423.
 578 [9] H. Durand, P. Christofides, Actuator stiction compensation via model pre-
 579 dictive control for nonlinear processes, AIChE Journal 62 (2016) 2004–
 580 2023.
 581 [10] H. Durand, P. Christofides, Empirical modeling of control valve layer
 582 with application to model predictive control-based stiction compensation,
 583 in: Proceedings of the 10th IFAC Symposium on Nonlinear Control Sys-
 584 tems, Marriott Hotel Monterey, CA, USA, 23–25 August, 2016, pp. 41–
 585 46.
 586 [11] N. Thornhill, A. Horch, Advances and new directions in plant-wide dis-
 587 turbance detection and diagnosis, Contr. Eng. Pract. 15 (2007) 1196–
 588 1206.
 589 [12] R. Bacci di Capaci, C. Scali, Review and comparison of techniques of
 590 analysis of valve stiction: From modeling to smart diagnosis, Chem. Eng.
 591 Res. Des. 130 (2018) 230–265.
 592 [13] Q. P. He, J. Wang, Valve stiction modeling: First-principles vs. data-drive
 593 approaches, in: Proceedings of the 7th American Control Conference,
 594 Baltimore, MD, USA, 30 June–2 July, 2010, pp. 3777–3782.
 595 [14] R. Bacci di Capaci, C. Scali, Process control performance evaluation in
 596 the case of frequent set-point changes with experimental applications,
 597 Can. J. Chem. Eng. 95 (2017) 1707–1720.
 598

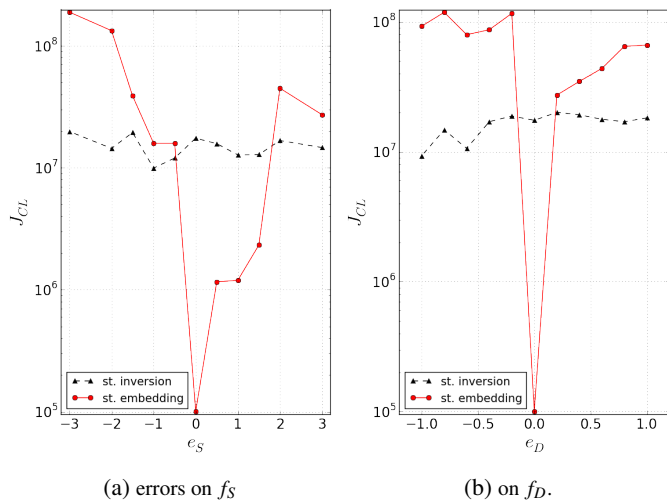


Figure 15: Effect of mismatch on stiction parameters

- 599 [15] C. Garcia, Comparison of friction models applied to a control valve, *Control Eng. Pract.* 16 (2008) 1231–1243.
- 600 [16] Q. P. He, J. Wang, M. Pottmann, S. J. Qin, A curve fitting method for detecting valve stiction in oscillating control loops, *Ind. Eng. Chem. Res.* 46 (2007) 4549–4560.
- 601 [17] M. Kano, M. Hiroshi, H. Kugemoto, K. Shimizu, Practical model and detection algorithm for valve stiction, in: *Proceedings of 7th IFAC DYCOPS, Boston, USA, 2004*, paper ID n. 54.
- 602 [18] S. L. Chen, K. K. Tan, S. Huang, Two-layer binary tree data-driven model for valve stiction, *Ind. Eng. Chem. Res.* 47 (2008) 2842–2848.
- 603 [19] G. Pannocchia, M. Gabiccini, A. Artoni, Offset-free MPC explained: novelties, subtleties, and applications, in: *Proceedings of 5th IFAC Conference on Nonlinear Model Predictive Control NMPC, Seville, Spain, 17–20 September, 2015*, pp. 342–351.
- 604 [20] R. Srinivasan, R. Rengaswamy, Approaches for efficient stiction compensation in process control valves, *Comput. Chem. Eng.* 32 (2008) 218–229.
- 605 [21] T. Wang, L. Xie, F. Tan, H. Su, A new implementation of open-loop two-move compensation method for oscillations caused by control valve stiction, in: *Proceedings of 9th IFAC ADCHEM, Whistler, BC, Canada, 7–10 June, 2015*, pp. 433–438.
- 606 [22] R. Bacci di Capaci, C. Scali, B. Huang, A revised technique of stiction compensation for control valves, in: *Proceedings of the 11th IFAC DYCOPS, Trondheim, Norway, 6–8 June, 2016*, pp. 1038–1043.
- 607 [23] L. Tang, J. Wang, Estimation of the most critical parameter for the two-movement method to compensate for oscillations caused by control valve stiction, *IEEE Transaction on Control Systems Technology* 24 (2016) 1869–1874.
- 608 [24] A. Stenman, F. Gustafsson, K. Forsman, A segmentation-based method for detection of stiction in control valves, *Int. J. Adapt. Control* 17 (2003) 625–634.
- 609 [25] M. Vaccari, G. Pannocchia, A multipurpose, easy-to-use Model Predictive Control design and simulation code, in: *Proceedings of the 4th European Conference on Computational Optimization EUCCO, Leuven, Belgium, 2016*, p. 136.
- 610 [26] K. H. Johansson, The quadruple-tank process: A multivariable laboratory process with an adjustable zero, *IEEE Transaction on Control Systems Technology* 8 (2000) 456–465.